09

Wavefront sensor for wide-aperture laser beams and its applications

© L.V. Volkova,[1] S.Y. Kazantsev,[2] A.Yu. Muzychka,[1] V.S. Skobeleva[1]

[1] Moscow Polytechnic University,
107023 Moscow, Russia
[2] Moscow Technical University of Communications and Informatics,
111024 Moscow, Russia
s.i.kazantsev@mtuci.ru

Received March 5, 2022
Revised April 6, 2022
Accepted April 6, 2022

The results of studies of a wavefront sensor based on the Talbot effect, in which a periodic grating made by laser printing is used, are presented. The optical characteristics of periodic gratings printed on polymer films exposed to a continuous radiation density of up to 0.9 W/cm^2 have been studied. The possibility of creating efficient configurable wavefront sensors for lasers in the visible and mid-IR spectral ranges is demonstrated.

Keywords: wavefront sensor, Talbot effect, wide-aperture laser beams, polymer films, periodic gratings.

DOI: 10.21883/TP.2022.09.54686.49-22

Introduction

The problem of wavefront (WF) control of wide-aperture beams is relevant for many applications of laser physics and atmospheric optics [1–3]. In addition, WF sensors can be used to control the shape of various lenses and mirrors that are part of complex optical systems with large transverse dimensions, which are used in surveillance systems [4,5]. The need to scan areas of mirror surfaces with transverse dimensions above 10 cm or the need for operational control of wide-aperture beams of high-power lasers in the mid-IR spectral range causes certain difficulties when using standard WF sensors (based on the Shack–Hartmann scheme) [5]. These difficulties are mainly related to the fact that in order to detect radiation with a wavelength greater than 3 μm, in wavefront sensors based on the Shack–Hartmann scheme, one has to use special optics and receiver arrays. Therefore, the approaches implemented, for example, in [6,7], even taking into account modern successes in the creation of wide-aperture optics from ZnSe and photodetectors for the spectral region 2–20 μm, lead to a significant increase in the device cost, which makes it unavailable for general use. At the same time, it is known that the approach based on the Talbot effect [8,9] can be successfully used to control the wavefront of high-power wide-aperture IR lasers. The Talbot effect is realized on wave beams of various nature, some examples are presented in the papers [10–12]. An important advantage of using interferometric techniques based on the Talbot effect is the absence of the need to use a large number of optical elements made from materials that must be transparent to the radiation under study. In the Talbot effect, the key element is a two-dimensional periodic grating, on which the diffraction decomposition of the wave front takes place, while the dimensions of such a grating can be quite large, which makes it possible to diagnose the active medium of lasers with a large working volume [9,13]. It is known that the Talbot interferometry technique is also effective for diagnosing gas-dynamic flows and measuring optical inhomogeneities of transparent media [5,14]. Therefore, this technique will be especially attractive for revealing inhomogeneities in transparent dielectrics or gas-discharge plasma [15]. However, the analysis using this technique of self-organizing plasma structures, described in the papers [16,17], revealed a number of problems. It turned out that the period of plasma structures, depending on the conditions (specific energy input, pressure and composition of the gaseous medium, the state of the electrode surface), changes greatly [16], as a result of which it becomes necessary to select the optimal period for the grating used in the Talbot interferometer. Periodic gratings, which were used in the experiments [9], were made of metal foil using a fairly complex photolithographic technology. It is obvious that the manufacture of a special metal grating for each new experiment is not advisable. Therefore, in the works [15,18] it was proposed to produce periodic gratings by laser printing on a polymer film, however, a detailed analysis of the material, quality and stability of the characteristics of printed periodic gratings was not carried out in [15,18]. The aim of this work was to study the possibility of using printed gratings in a wavefront sensor to analyze optical inhomogeneities of the medium, as well as to estimate the applicability limit of both the polymer material itself and the laser printer ink used to create a periodic grating.

1. Experimental unit and research technique

In the Talbot effect, plane coherent waves of laser radiation sources are decomposed on a two-dimensional grating of randomly shaped but periodically arranged holes into

spatial harmonics propagating at multiple angles, which, as a result of interference in the near Fresnel zone, reproduce the intensity distribution on the grating at distances determined by the expression [17]:

$$r_n = \frac{2p^2 n}{\lambda}. \quad (1)$$

Here $p \gg \lambda$; r_n — distance from grating to nth reproduction plane, p — grating period, λ — radiation wavelength, $n = 1, 2.3 \ldots$. The intensity distribution in the reproduction planes has a lattice-like periodic structure when the WF is flat or spherical. With a convex WF, the periods in the reproduction plane increase, and with a concave they decrease relative to the grating period. Thus, an increase in the period in a certain region of the aperture of a plane beam that has passed through a section of the medium indicates the appearance in this region of an optical inhomogeneity of the type of a diverging lens, a decrease — that of a focusing lens. Measuring the displacement of coordinates of contrast spots in the distribution of the intensity of talbograms distorted by WFs in the reproduction planes is the basis of the WF sensor. Local WF slopes Δy are measured in the reproduction planes. In the optical wedge approximation [9]:

$$\Delta y = \frac{\sqrt{\Delta x^2 + \Delta y^2}}{r_1}, \quad (2)$$

where $\Delta x, \Delta y$ — shifts of spot coordinates in a rectangular coordinate system. The normal deviation of the WF is $\Delta z = p\Delta y$. The WF curvature radius R is determined in the parabolic approximation from the change in the periods Δp in the reproduction plane [5]:

$$R = \frac{pr_1}{\Delta p}, \quad (3)$$

where Δp — period change in the playback plane.

A feature of Talbot interferometry is that to obtain information about the shape of the WF, detailed measurements of the spatial distribution of the radiation intensity are not required. It suffices to measure only the coordinates of the centers of the contrasting radiation spots on the talbograms, and the size of the spots can be chosen to be small compared to the period. This reduces the requirement for the dynamic range of the screens and makes it easier to automatically read the coordinates.

An experimental setup for studying the characteristics of a WF sensor based on the Talbot effect, as well as its applications for the analysis of optical inhomogeneities in transparent media, is shown in Fig. 1. Attention should be paid to the key element of the entire setup — periodic grating (PG), whose properties were studied in detail in our work. The grating was printed on a polymer film using an HP LaserJet Pro MFP M132mw laser printer, after which it was installed in a special cassette, which in most experiments consisted of flat glass plates, between which this polymer film was clamped, or mounted on

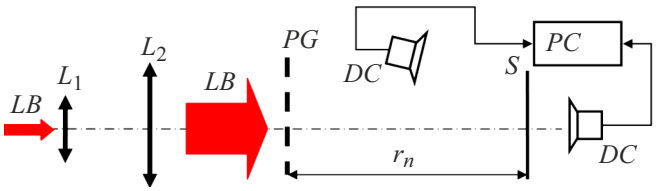

Figure 1. Experimental setup. LB — laser beam; L_1, L_2 — lenses forming a telescope; PG — periodic grating; S — screen for registration of talbograms; DC — digital camera; PC — personal computer for processing talbograms.

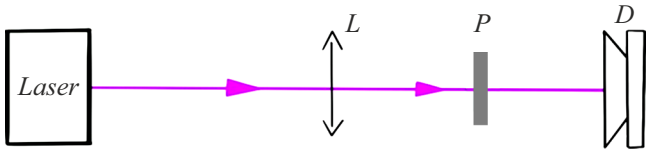

Figure 2. Experimental unit for studying the effect of laser radiation on the properties of printed periodic gratings: L — lens; P — polymer sample; D — thermal sensor.

a frame [18]. Further, the spectral properties of PET films, which were used to fabricate gratings, were studied. The absorption spectra of the films were recorded after exposure to various doses of continuous laser radiation with wavelengths $\lambda = 405$, 530, and 633 nm. In addition, in special experiments, instead of laser irradiation, the films were subjected to heat treatment. Commercial Mylar films (thickness 30 μm), as well as films from the firms folex IMAGING and LOMOND, thickness 60 μm were taken as polymer samples. The laser radiation power density on the film varied within 0.02–0.9 W/cm^2, the inhomogeneity of the laser radiation density in the irradiation spot on the film did not exceed 10% relative to its average value. The irradiation time varied from 1 to 60 min. The absorption spectra of the samples were recorded on a „SHIMADZU“ UV-1280, spectrophotometer, and in the spectral range 2–25 μm the transmission dependences of these films were recorded using an AF-3 IR Fourier transform spectrometer [19]. The study of the structure of laser paint was carried out using a microscope.

Figure 2 shows a diagram of an experimental unit in which changes in the optical characteristics of films were studied after exposure to high-power laser irradiation. The beam from the laser facility through a lens (L) hit a polymer sample (P). The temperature of the irradiated surface was recorded using a thermal sensor (D).

2. Study results and their discussion

Periodic gratings printed by a laser printer on films with a period of 0.3 to 1.5 mm of various geometries were studied. The studies revealed the high sensitivity of the WF sensor we assembled and the possibility of its application for monitoring the optical homogeneity of the laser beam

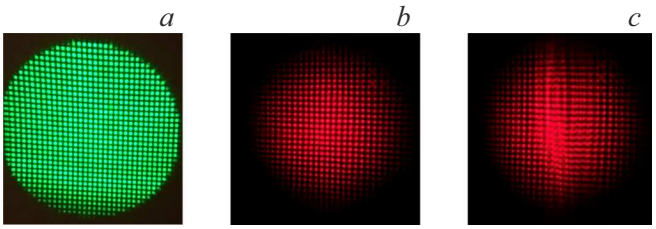

Figure 3. Photographs of talbograms in the reproduction plane: *a* — a green laser beam with a diameter of 50 mm was used; *b* — red laser; *c* — red laser, laser beam path perturbed by heat flow (lighter flame).

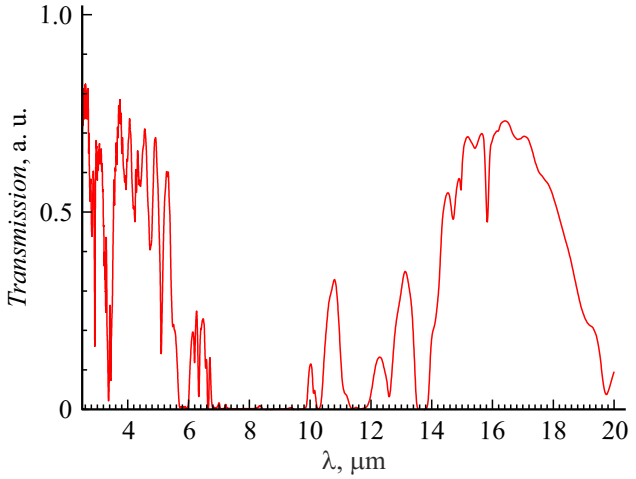

Figure 4. Transmission spectra of a PET sample without ink from a printer.

path. Figure 3 shows typical talbograms obtained on an experimental bench in the second reproduction plane: in Figure 3, *a, b* the beam path was not perturbed; Fig. 3, *c* shows a talbogram obtained when the laser beam passed at a distance of 5 cm above the lighter flame. It can be seen that a change in the refractive index in hot air caused a shift in the interference maxima in the reproduction plane and a loss of picture clarity, which was also reliably recorded during high-speed video recording [13]. As can be seen from Fig. 3, *c*, the shift of interference maxima in the talbogram under strong perturbations of the optical density of the medium can exceed the grating period; in this case, the very fact of wavefront distortions is fixed, and for numerical estimates of these distortions, a grating with a long period should be used. During the experiments described above, the density of laser radiation on a periodic grating did not exceed 8 mW/cm^2. And at such an intensity of irradiation, gratings printed on lavsan film practically did not change their properties during the entire cycle of research. This is more than 10 months with continuous exposure for one day to laser radiation with $\lambda = 530$ and 633 nm no more than 3 h at room temperature $T = 18-28$°C. Therefore, these gratings and the materials on which they were printed were exposed to more severe laser radiation. As a result, it was found that at an irradiation density below 0.5 mW/cm^2 of both green and violet lasers, no significant changes occurred either in the structure of the polymer or in the laser paint deposited on the polymer. In this case, the temperature on the sample surface, according to the thermal sensor data, did not exceed 30–32°C. Figure 4 shows the transmission spectrum of 60 μm PET in the mid-IR region of the spectrum, from which one can see the characteristic transparency regions of the material, where periodic gratings printed on this polymer can work. Long-term irradiation (1 h) of PET at maximum power values up to 0.5 W/cm^2 did not lead to the appearance of absorption bands of the polymer in the visible and near-IR spectral regions (Fig. 5), which indicates the stability of PET in these spectral ranges. Thus, the polymer matrix under these conditions cannot affect the performance of the talbogram.

An important detail of the talbogram is a periodic grating applied to the polymer using a laser printer [18], in which a coloring powder (toner) with a granular structure is used to create an image. A toner granule (Fig. 6) consists of a paraffin core *1* surrounded by a polymer shell *2* containing a pigment and various additives (magnetic, polyethylene

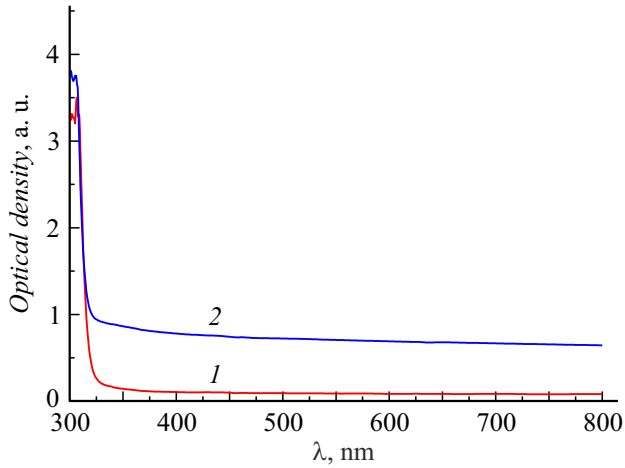

Figure 5. Absorption spectra of PET samples before (*1*) and after (*2*) irradiation with a $P = 0.9$ W/cm^2 violet laser for 60 min at room temperature.

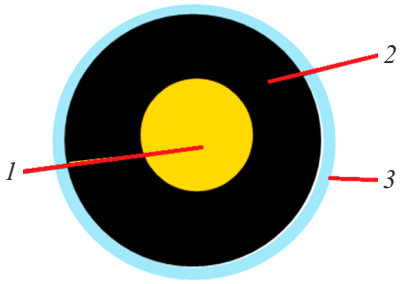

Figure 6. Schematic representation of a granule of laser paint (toner): *1* — core; *2* — polymer shell; *3* — special layer to prevent sticking of granules.

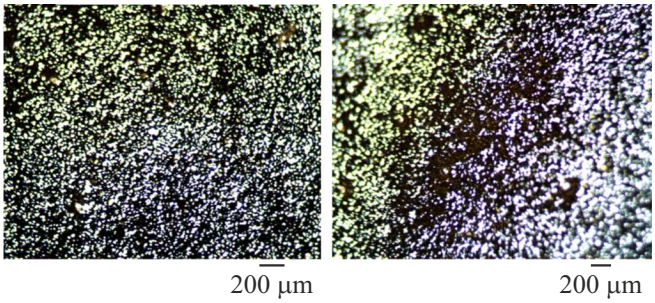

Figure 7. Image of a fragment (PET + paint) under a microscope before (*a*) and after (*b*) irradiation with a violet laser ($P = 0.9\,\mathrm{W/cm^2}$).

or polypropylene as a modifier, etc.), and also surface additives to prevent sticking of the granules *3*. Currently, in the production of toners, the polymer shell is made from polyesters or styrene-acrylic polymers. Fig. 7 shows images of a fragment of a PET sample on which the grating is printed. The images were taken under magnification with a microscope. Fig. 7, *a* shows that even after passing through the thermal rollers, not all the toner granules have melted, as indicated by white areas ranging in size from 5 to $30\,\mu$m. With long-term irradiation of the sample with a green laser ($P = 0.4\,\mathrm{W/cm^2}$), as well as with a violet laser at low and medium power ($P < 0.5\,\mathrm{W/cm^2}$) no changes in the structure of the paint were observed. However, irradiation of the sample with powerful violet laser beams ($P = 0.9\,\mathrm{W/cm^2}$) for 2–3 min led to a decrease in the size of the gaps and an increase in the areas filled with pigment (soot) formed as a result of the thermal action of the laser on the remaining unmelted paint granules. According to the thermal sensor data, the temperature on the surface of the sample increased to $T = 70$–80°C under this effect. Fig. 7, *b* shows the place where the laser beam acts on the sample (dark area). For talbograms with a grating period of about $400\,\mu$m, such an effect can lead to a significant deterioration in transparency. With an increase in the irradiation time to 10–15 min, both a change in the color of the paint (the appearance of a dark yellow spot) and a decrease in the elasticity of the polymer film were observed. These facts are direct evidence of the occurrence of thermal-oxidative processes leading to the destruction of the polymer matrix and laser ink.

Conclusion

Thus, for laser sources in the visible range, periodic gratings in the wavefront sensor can be printed by a laser printer on a transparent lavsan film. Research has demonstrated the significant advantages of the Talbot effect wavefront sensor for analyzing dynamic perturbations in optical density in transparent materials as well as airways. It is shown that in the spectral intervals 0.4–$2\,\mu$m, 2.6–$5\,\mu$m, 10.5–$11.2\,\mu$m, 12.6–$13.4\,\mu$m and 15–$18\,\mu$m industrial polyethylene terephthalate films can be effectively used as a matrix for talbograms. It should be noted that the absence of special expensive optics, the possibility of increasing the transverse size of the test beam above 10 cm, and the use of cheap digital video cameras for recording talbograms make the method based on the Talbot effect attractive for various applications, in particular, for analyzing the characteristics of plasma formations in volume discharge [15,16], analysis of gas dynamic flows [5,10], for wavefront control of pulsed chemical lasers [9] or medicine [20] . The limits of applicability of polymer talbograms are determined by the thermal effects that occur when samples are irradiated with a laser, and can be adjusted by selecting the exposure conditions and choosing a special paint. It is obvious that the cheap technique for fabricating periodic gratings for realizing the Talbot effect, described in this paper, makes it possible to carry out both demonstration experiments in educational laboratories [21] and to explore new applications of this effect in quantum optics and cryptography with minimal costs, which are of great interest lately [22–24].

Conflict of interest

The authors declare that they have no conflict of interest.

References

[1] I.V. Galaktionov, A.V. Kudryashov, Yu.V. Sheldakova, A.A. Bialko, J. Borsoni. Kvant. elektron., **47** (1), 32 (2017). DOI: 10.1070/QEL16061
[2] L.V. Antoshkin, N.N. Botygina, L.A. Bolbasova, O.N. Emaleev, P.A. Konyaev, E.A. Kopylov, P.G. Kovadlo, D.Yu. Kolobov, A.V. Kudryashov, V.V. Lavrinov, L.N. Lavrinova, V.P. Lukin, S.A. Chuprakov, A.A. Selin, A.Yu. Shikhovtsev. Optika atmosfery i okeana, **29** (11), 895 (2016) (in Russian). DOI: 10.15372/AOO20161101
[3] Lejia Hu, Shuwen Hu, Wei Gong, Ke Si. Opt. Lett., **45** (13), 3741 (2020). DOI: 10.1364/OL.395579
[4] T.S. Piskunov, N.V. Baryshnikov, I.V. Zhivotovskii, A.A. Sakharov, V.A. Sokolovskii. Opt. Spectr. **127** (4), 639 (2019). DOI: 10.1134/S0030400X19100217
[5] A.S. Koryakovsky, V.M. Marchenko, A.M. Prokhorov. Trudy IOFAN, **7**, 33 (1987) (in Russian).
[6] M.A. Glukhov, A.I. Golubev, M.O. Koltygin, R.S. Kuzin, A.N. Manachinsky, F.A. Starikov. Trudy RFYATS-VNIIEF. **20**, 300 (2015) (in Russian).
[7] A.V. Kotov, S.E. Perevalov, M.V. Starodubtsev, R.S. Zemskov, A.G. Aleksandrov, I.V. Galaktionov, A.V. Kudryashov, V.V. Samarkin, A.A. Soloviev. Kvant. elektron., **51** (7), 593 (2021) (in Russian). DOI: 10.1070/QEL17542
[8] D.V. Podanchuk, A.A. Goloborodko, M.M. Kotov, A.V. Kovalenko, V.N. Kurashov, V.P. Dan'ko. Appl. Opt., **55** (12), B150 (2016). DOI: 10.1364/AO.55.00B150
[9] A.B. Ignat'ev, S.Yu. Kazantsev, I.G. Kononov, V.M. Marchenko, V.A. Feofilaktov, K.N. Firsov. Quant. Electron., **38** (1), 69 (2008). DOI: 10.1070/QE2008v038n01ABEH013546
[10] A.S. Boreisho, A.S. Koryakovsky, V.M. Marchenko, A.V. Morozov, V.E. Sokolov. ZhTF **55** (10), 1943 (1985) (in Russian).

[11] J. Wen, Y. Zhang, M. Xiao. Adv. Opt. Photon., **5** (1) 83 (2013). DOI: 10.1364/AOP.5.000083
[12] A.N. Morozov, L.R. Salbieva, B.G. Skuibin, E.V. Smirnov. JETP Lett., **107**, 355 (2018). DOI: 10.1134/S0021364018060085
[13] A.S. Koryakovskii, V.M. Marchenko. Soviet J. Quant. Electron., **10** (5), 598 (1980).
[14] I.G. Palchikova, S.S. Popova, S.V. Smirnov. Komp'yuternaya optika, **20**, 60 (2000) (in Russian).
[15] S.N. Andreev, S.Y. Kazantsev, A.Y. Muzychka. *Frontiers in Optics + Laser Science 2021* (Optica Publishing Group, 2021), JTh5A.121. DOI: 10.1364/FIO.2021.JTh5A.121
[16] V.V. Apollonov, S.Y. Kazantsev. Tech. Phys. Lett., **45**, 443 (2019). DOI: 10.1134/S106378501905002X
[17] V.V. Apollonov, S.Y. Kazantsev. Bull. Lebedev Phys. Institute, **46** (5), 161 (2019). DOI: 10.3103/S1068335619050038
[18] I.V. Gubanova, S.Yu. Kazantsev, A.Yu. Muzychka. *Materialy Vserossiyskoy nauchno-prakticheskoy konferentsii* (Moskva, Rossiya, 2021), c. 351–355 (in Russian).
[19] A.A. Ionin, D.V. Badikov, V.V. Badikov, I.O. Kinyaevskiy, Yu.M. Klimachev, A.A. Kotkov, A.Yu. Kozlov, A.M. Sagitova, D.V. Sinitsyn. Opt. Lett., **43** (18), 4358 (2018). DOI: 10.1364/OL.43.004358
[20] S. Agarwal, V. Kumar, C. Shakher. *Imaging and Applied Optics 2017* (Optica Publishing Group, 2017), JTu5A.27.3. DOI: 10.1364/3D.2017.JTu5A.27
[21] V.P. Kandidov, A.M. Korolkov. Fizicheskoye obrazovaniye v vuzakh, **4** (3), 99 (1998) (in Russian).
[22] Lin Li, Haigang Liu, Chen Xianfeng. Opt. Lett., **46**, 1281 (2021). DOI: 10.1364/OL.416988
[23] Hu Jianqi, Brés Camille-Sophie, Chen-Bin Huang. Opt. Lett., **43**, 4033 (2018). DOI: 10.1364/OL.43.004033
[24] Jingjing Wu, Jicheng Wang, Yanguang Nie, Lifa Hu. Opt. Express, **27**, 35096 (2019). DOI: 10.1364/OE.27.035096